International Journal of Advanced Science and Research
www.allsciencejournal.com
ISSN: 2455-4227
Received: 22-04-2022, Accepted: 07-05-2022, Published: 23-05-2022
Volume 7, Issue 2, 2022, Page No. 15-22

Mathematical and numerical study for a bioglass bioactivity degradation

Aymen Hadji[1], Fatma Zohra Nouri[2]
[1] Department of Pharmacy, Faculty of Medical Sciences, University of Batna 2, Batna, Algeria
[2] Mathematical Modeling and Numerical Simulation Research Lab, Faculty of Sciences, Badji Mokhtar University, Annaba, Algeria

Abstract
In this work we develop a mathematical model, based on a system of reaction-diffusion equations, to analyse the dissolution and bioactivity for a bio-glass. The development of porous bioactive glasses is part of a multidisciplinary task. This family of substitutes is particularly adapted to regenerative medicine and suitable for many applications such as prolonged-release drugs. For example in pharmacology, the development of bioactive systems have shown that the release of drugs from the synthesized porous bio-glasses is controlled by a diffusion mechanism, such as a dissolution-precipitation process, due to the porosity criteria. Here we first show the well-posedness of the derived mathematical model, then we propose a numerical framework using a finite volume scheme to show useful results in real applications.
2020 Subject Classification. Primary 97M10, 97M60; Secondary 65L60, 65N12.

Keywords: bioactive glass, mathematical modelling, finite volumes

Introduction

The ternary SiO_2-CaO-P_2O_5 systems was first realized by Michelina Catauro (2015) [2], using tetraethyl orthosilicate (TEOS; Si $(OC_2H_5)_4$) precursor. In the work by Hadji *et al* (2018) [6], the same system was studied, using aerosol SiO_2 commercial precursor and varying the percentage of added molar in the considered composition.
The preparation was realised via the sol-gel method, which has the advantage of ensuring good homogenisation of reactants and preventing phase separation (see also) [2, 3, 4, 5, 8, 9, 12, 13].
The particularity of this ternary system is the bioactivity and the porosity leading to many applications, for example, the synthesized porous bio-glasses are controlled by diffusion mechanism. Furthermore bioactive glasses produce a series of physico-chemical reactions at the material/bone tissue interface that lead to the formation of a calcium phosphate layer.
The evolution of this layer gives it a structure similar to that of the mineral phase of the bone, which allows an intimate bond between the bioactive glass and the host tissues. It is this bond which characterizes the bioactivity of the material.
The experimental evaluation of the degradation of bioactive glasses in contact with body fluid requires long-term *in vitro* tests. Unfortunately very few works have been developed to numerically analyze degradation and dissolution of biomaterials. Wang *et al*. (2009) [17] and J.A. Sanz-Herrera *et al* (2011) [14] presented models to analyze degradation of biopolymers. In this paper, a mathematical model is proposed to numerically analyze the dissolution and bioactivity for the $SiO_2CaOP_2O_5$ bioglass, in order to account for the micro structural evolution as consequence of degradation, using simple and low cost numerical schemes. The work is organised as follows: Section 2 is just a reference of the experimental results. Section 3 is devoted to the equations setting, while in sections 4 and 5 we present the proposed model and its mathematical analysis. In section 6, we give the numerical approach including the discretisation, the algorithm, results and comments; and finishing by concluding remarks resumed in section 7.

Experimental Results

In the interest of obtaining a stoichiometric mixture, the ratio of the precursors used were:
1. Sample I: SiO_2 (50%); $CaNO_3$: $4H_2O$ (50%) and Na_2HPO_4 (0%)
2. Sample II: SiO_2 (73%); $CaNO_3$: $4H_2O$ (22%) and Na_2HPO_4 (5%)
3. Sample III: SiO_2 (73%); $CaNO_3$: $4H_2O$ (17%) and Na_2HPO_4 (10%):

For details on the methods and techniques used to get the resulting amorphous bioglass SiO_2 $CaOP_2O_5$, together with their chemical bonding, structural and morphological properties, the reader is referred to Hadji *et al* (2018) [6].

Modeling Bioactivity and Dissolution

Problem Description

This section is addressed to the equations modelling the dissolution of the bioactive glass. The model is rationally based on the chemistry and underlying phenomena that take place once a bioactive glass B sample is immersed in a simulated body fluid denoted by S, representing usually the first test carried out on biomaterials to detect the formation of hydroxycarbonate apatite HA, which should lead to strong bond to bone tissue (see Hench, 1998 [7] and references therein).

Once the biomaterial is flooded by S, the bio-reactivity leads to a number of reactions, which may be resumed through a sequence of five steps consecutively:

1. The ions are progressively released at the solution surface S,
2. the corresponding increase in local pH promotes breaking of surface Si-O-Si bonds and release of soluble silica to the solution S,
3. some of the surface silanol groups formed in steps (1) and (2) condense to form a hydrated silica-rich layer on the surface, depleted in modifier cations,
4. calcium and phosphate ions are released through the surface silica layer, and incorporate other Ca_2^+ and PO_4^{3-} from the solution S to form an amorphous calcium phosphate phase deposited on the surface, and
5. the latter amorphous film incorporates additional carbonate ions from solution and crystallizes to HA.

In this study, we consider both the process of bioactivity and dissolution, according to the following main species (See Figure 1.):

1. S [mol/m3] which is an aqueous solution in contact with the biomaterial.
2. Bioactive glass B [mol/m3] representing the overall constituent of the scaffold and reacting with S.
3. Reactant aqueous solution R [mol=m3] which expresses the overall dissolved products (cations and anions) resulting from the reaction between B and S.
4. Precipitate P [mol/m3] which constitutes the overall nucleated products deposited on the biomaterial surface.

According to these steps, we can write down the following model equations.

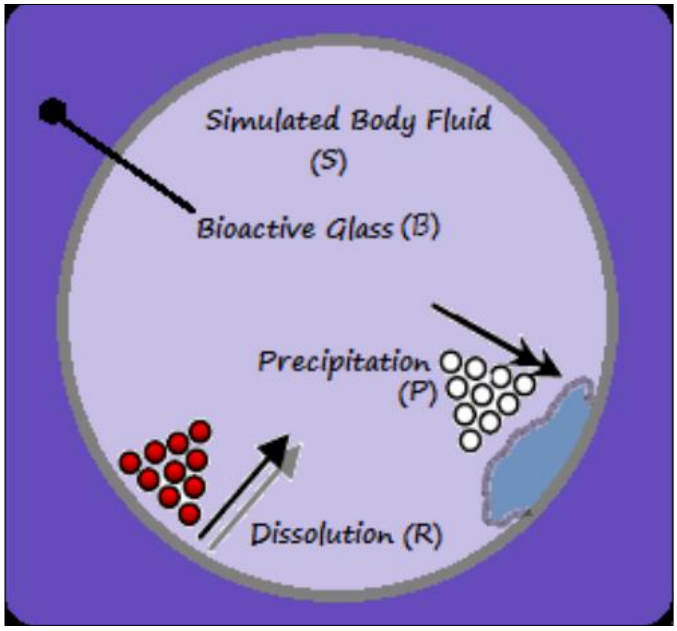

Fig 1: Different species and their implication in the different reactions.

Equation for B's dissolution

Assuming that the biomaterial is homogeneous and as a consequence of the micropores formed during the fabrication of the scaffold (Chen *et al*., 2006a [3]), the S and R can diffuse into the biomaterial so that we can write

$$M_{sd}\, S(aq) + M_b\, B(ac) \rightarrow M_{rd}\, R(aq) + O_d \tag{3.1}$$

The coefficients M_{sd}; M_b and M_{rd} are the molar proportions of the involved species in the dissolution reaction and O_d represents other species involved in the dissolution reaction scaffold. Note that equation (3.1) does not only apply on the surface but on the entire domain.

Bioactivity-Dissolution Model

Let us consider a biomaterial domain D(x) and a dissolution rate coefficient k_d [1/s]. Note that the formation rate of R only depends on B concentration such that $\frac{dRd}{dt} = \mathbf{Kd\ S\ H[B]}$, with $\mathbf{H[B]} = \begin{cases} \mathbf{1} & \mathbf{if\ B > 0} \\ \mathbf{0} & \mathbf{if\ B = 0} \end{cases}$ that denotes the Heaviside function taking into account the stechiometry of equation (3.1) in terms of the limiting reagent (for more details the reader is referred to Van Noorden and Pop, 2008 [16]).

Hence we can write the rate reaction equations of B and S dissolution as

$$\frac{dB}{dt} = -\frac{M_{rd}}{M_b}\frac{dR_d}{dt}. \qquad in\ D(x),$$

$$\frac{dS_d}{dt} = -\frac{M_{rd}}{M_{sd}}\frac{dR_d}{dt}. \qquad in\ D(x). \tag{4.1}$$

Here S_d and R_d are the consumption of S and R in the dissolution process, respectively.

If we assume that dimension is driven by the Fick's law both for S and R, and a mass transfer over an infinitesimal control volume, we write

$$\begin{cases} \frac{dB}{dt} = -\frac{M_{rd}}{M_b}\frac{dR_d}{dt}, & in\ D(x), \\ \frac{dS}{dt} = -D_s\ \triangle S + \frac{dS_d}{dt}. & in\ D(x), \\ \frac{dR}{dt} = -D_r\ \triangle R + \frac{dR_d}{dt}. & in\ D(x). \end{cases} \tag{4.2}$$

By using the fact that $\frac{dR_d}{dt} = K_d\ \mathbf{S\ H[B]}$, we can write the model as a reaction-diffusion system in the form

$$\begin{cases} \frac{dB}{dt} = -\frac{M_{rd}}{M_b} K_d\ \mathrm{S\ H[B]}, & in\ D(x), \\ \frac{dS}{dt} = -D_s\ \triangle S - \frac{M_{rd}}{M_{sd}} K_d\ \mathrm{S\ H[B]} & in\ D(x), \\ \frac{dR}{dt} = -D_r\ \triangle R + K_d\ \mathrm{S\ H[B]}. & in\ D(x). \end{cases} \tag{4.3}$$

Where D_S and Dr are the diffusion coefficients of S and R, respectively, in the biomaterial (assumed as constant as a first approach). System (4.3) define the proposed model available to analyse bioactivity and dissolution in bioactive-glasses.

This system is completed by initial and boundary conditions.

Initial Conditions

The initial conditions to be considered are

$$S_{t=0} = S_0,\ R_{t=0} = 0,\ B_{t=0} = B_0. \tag{4.4}$$

Boundary Conditions

Due to the reactions at the boundary S - B, the concentration of S decreases and we have:

1. S diffuses along the solution much faster than in both the biomaterial and the typical reaction times
2. S is plentiful and hence the concentration of S is constant, i.e. oversaturated along the biomaterial B.

For the reactant, a mass conservation equation is considered at the S - B surface. As a consequence of erosion and precipitation reactions on the surface, it is noted that the biomaterial boundary Γ (surface of B) is changing with time and this is due to the B bioactivity, hence we have

$$S(x;t) = 1\ \ and\ \ R(x;t) = g \quad on\ \ \Gamma. \tag{4.5}$$

Dimensionless

We propose the following change of variables

$$x^* = \frac{x}{l};\ t^* = k_d t;\ S^* = \frac{S}{S_0};\ B^* = \frac{B}{B_0};\ R^* = \frac{\boldsymbol{R}}{S_0};\ D_S^* = \frac{D_S}{k_d}\ and\ D_r^* = \frac{D_r}{k_d}\ \text{to get}$$

$$\frac{dB^*}{dt^*} = -\frac{M_{rd}}{M_b}\ S^*\ \mathrm{H}[B^*]\ \ \text{in D}(x^*),\ \ B^*_{t^*=0} = B_0^*, \tag{4.6}$$

$$\begin{cases} \frac{\partial S^*}{dt^*} = -D_S^*\ \triangle S^* - \frac{M_{rd}}{M_{sd}}\ S^*\ \mathrm{H}[B^*]\ \ \text{in D}(x^*),\ \ S^*_{t^*=0} = 1, \\ \frac{\partial R^*}{dt^*} = -D_r^*\ \triangle R^* + S^*\ \mathrm{H}[B^*]\ \ \text{in D}(x^*),\ \ R^*_{t^*=0} = 0, \\ \text{with appropriate boundary conditions on}\ \ \Gamma, \end{cases} \tag{4.7}$$

Where l is the specimen size. Let us derive the boundary conditions for S^* and R^*. For S^*;we assume that: first the simulated body fluid diffuses along the solution much more faster than in the biomaterial, and secondly it is abundant and hence no S^* depletion is considered along the solution. Therefore, we consider that the simulated body fluid concentration is constant (oversaturated) along the biomaterial surface Γ, i.e.

$$S^*(x^*, t^*) = 1 \quad on \ \Gamma(x^*) \tag{4.8}$$

To get boundary conditions for R^*, we note that the biomaterial boundary $\Gamma(x^*)$ is changing with time due to the bioactivity of the glass. It we denote by T^* the instant time when a point becomes a boundary point, we can write

$$R^*(x^*, T^*) = \begin{cases} \dfrac{\partial R^*}{dt^*} = S^*.\mathrm{H}[B^*] \ - \dfrac{M_b}{M_{rd}} \ k_d.S^*.R^* \\ or \ \dfrac{\partial R^*}{dt^*} = \mathrm{H}[B^*] \ - \dfrac{M_b}{M_{rd}} \ k_d.R^* \ on \ \Gamma(x^*) \\ R^*(x^*, T^*) = \begin{cases} 0, & T^*(x^*) = 0 \\ R^*_{T^*}(x^*), & T^*(x^*) > 0, \end{cases} \quad \forall\, x^* \in \Gamma(x^*) \end{cases} \tag{4.9}$$

Problem (4.9) is then solved to give the following boundary condition

$$R^*(x^*, T^*) = R^*_{T^*}(x^*)e^{-C_d^*\,\tau} + \frac{1}{C_d^*}\mathrm{H}[B^*](1 - e^{-C_d^*\,\tau}), \quad \text{on} \quad \Gamma(x^*)$$
$$\text{where } C_d^* = \frac{M_b}{M_{rd}} \ k_d \ \ and \ \tau = t^* \ - T^*(x^*). \tag{4.10}$$

To show the well posedness of this problem we use a weak formulation, for more details the reader is referred to Nouri [10].

Numerical Approach

Numerical Discretisation

To solve the system of equations ((4.6)-(4.7)) together with the initial conditions (4.4) and the boundary conditions (4.8) and (4.10), we consider a finite difference and a finite volume schemes for the time and the space variable discretisations, respectively. It should be pointed out that the disappearance, and new layer formation, due to the dissolution process, can be easily simulated by removing and adding elements, respectively.

Finite Volume Approximation

In this section we study the space approximation of solutions to the derived model (4.7) in the discrete finite volume framework. This family of schemes allows very general meshes and deals with the main properties of the physical features of the treated problems (see [1, 10] and references therein). The domain $\mathrm{D}(x)$ is discretised by a non-structured stitch meshing T_h. We introduce the following notation:

- Let $|K|$ denote the cell K surface, $N(K)$ the set of triangles having a common side with K.
- Let $e_{K,L}$ be the common side of the triangles K and L; and $n_{K,L}$ be the normal oriented from K towards L.
- $n_{e,i}$ is the external normal corresponding to the part of e_i at Γ.
- Let Z_h be the set of sides of T_h and Z_h^* be the set of interior sides.
- For a given side e, let us denote by M and N the extremities of e, by W and E the two triangles where e, where $e = W \cap E$; by $\aleph_e$ the diamond cell associated with e given by connecting the centres of gravities of the cells W and E with M and N.
- $((\varepsilon_i)_{i=1,4})$ are the four segments forming the border of $\aleph_e$.
- $n_e = \frac{1}{|\varepsilon_i|}(\mu_{x_i}, \mu_{y_i})$ is the normal on ε_i outgoing of $\aleph_e$.

For a given node N, $V(N)$ is the set of triangles with this node in common. For the numerical resolution (4.7) will be discretised as follows.

Discretisation

Let K be a cell of T_h, we integrate (4.7) on K to get

$$\begin{cases} \int_K \frac{\partial S^*}{\partial t^*} dx = -D_S^* \int_K div(\nabla S^*) dx - \frac{M_{rd}}{M_{sd}} \int_K S^* H[B^*] dx, \\ \int_K \frac{\partial R^*}{\partial t^*} dx = -D_r^* \int_K div(\nabla R^*) dx + \int_K S^* H[B^*] dx, \end{cases}$$

Where the operator $div(v) = \sum_{i=1}^{d} \frac{\partial v_i}{\partial x_i}$ (d is the dimension of the domain). By applying the divergence theorem, we have

$$\begin{cases} \int_K^{\square} \frac{\partial S^*}{\partial t^*} dx = -D_S^* \int_{\partial K}^{\square} \nabla S^* \, n_K d\sigma - \frac{M_{rd}}{M_{sd}} \int_K^{\square} S^* \, H[B^*] dx, \\ \int_K^{\square} \frac{\partial R^*}{\partial t^*} dx = -D_r^* \int_{\partial K}^{\square} \nabla R^* \, n_K d\sigma + \int_K^{\square} S^* \, H[B^*] dx, \end{cases} \quad (5.1)$$

∂K can be decomposed into edges e, therefore we obtain

$$\begin{cases} \int_K^{\square} \frac{\partial S^*}{\partial t^*} dx = -D_S^* . \sum_{e \in N(K)} \left(\int_e^{\square} \nabla S^* \, n_{K,e} d\sigma \right) - \frac{M_{rd}}{M_{sd}} \int_K^{\square} S^* \, H[B^*] dx, \\ \int_K^{\square} \frac{\partial R^*}{\partial t^*} dx = -D_r^* . \sum_{e \in N(K)} \left(\int_e^{\square} \nabla R^* \, n_{K,e} d\sigma \right) + \int_K^{\square} S^* \, H[B^*] dx, \end{cases} \quad (5.2)$$

This implies that

$$\begin{cases} \int_K^{\square} \frac{\partial S^*}{\partial t^*} dx = -D_S^* . \sum_{e \in N(K)} F_{K,e} - \frac{M_{rd}}{M_{sd}} \, |K| S^* \, H[B^*], \\ \int_K^{\square} \frac{\partial R^*}{\partial t^*} dx = -D_r^* . \sum_{e \in N(K)} G_{K,e} + |K| . S^* \, H[B^*], \end{cases} \quad (5.3)$$

where $F_{K,e} = \int_e \nabla S^* n_{K,e} d\sigma$ and $G_{K,e} = \int_e \nabla R^* n_{K,e} d\sigma$ are the numerical flows that are approximated by $F_{K,e} = \nabla_e S^* |e|$ and $G_{K,e} = \nabla_e R^* |e|$, where e is the side of the stitch meshing and $n_{K,e}$ is the normal of e outgoing from K, while ∇_e is the approximation of the gradient of S^* or R^* on the side e.

The construction of the approached gradient on e is done by the so-called Green-Gauss method see [1]. It consists of approaching the gradient by its means on a co-volume in the form of a diamond constructed around the side e. We write

$$\nabla_e = \frac{1}{|X_e|} \sum_{\varepsilon \in \partial X_e} \frac{1}{2} \big((p(x) N_1(\varepsilon) + p(x) N_2(\varepsilon) \big) |\epsilon| \, n_\varepsilon, \quad (5.5)$$

where X_e is the diamond cell associated with e, and $N_1(\varepsilon)$, $N_1(\varepsilon)$ are the extremities of ε, one of the four segments forming ∂X_e (the boundary of X_e and n_ε is the unit normal vector. The values of ρ at the centers W and E are P_W and P_E, while the values at nodes M and N are interpolated on the boundary and denoted by P_M and P_N. Hence at each node we have

$$P_M = \sum_{K \in V(M)} y_K(M) p_K \;\; and \;\; P_N = \sum_{K \in V(N)} y_K(N) \quad (5.6)$$

where $V(M)$ and $V(N)$ are the set of triangles sharing the node M or N, p_K is the value of p at the center of the cell K and $y_K(M)$ and $y_K(M)$ are the interpolation weights.

Error Analysis

Theorem 1: Assume that S^* belongs to $H^{\frac{3}{2}}(\Omega)$ (Ω is the domain $D(x)$). Then the following estimates hold

$$\|S^* - S_K^*\|_{H^{\frac{3}{2}}(\Omega} \leq C_1 \left(inf_{S_K^* \in N(K)} (\|S^* - S_K^*\|_{H^{\frac{3}{2}}(\Omega} + \|S^* - S_K^*\|_{L^2(\Omega)}) \right) \quad (5.7)$$

$$\|R^* - R_K^*\|_{H^1(\Omega)} \leq C_2 . inf_{S_K^* \in N(K)} \begin{pmatrix} \|R^* - R_K^*\|_{H^1(\Omega)} + \|S^* - S_K^*\|_{H^{\frac{3}{2}}(\Omega} \\ + \|S^* - S_K^*\|_{L^2(\Omega)} \end{pmatrix} \quad (5.8)$$

The proof of these results arise from the problem well posedness. Hence we can state the final estimate which arise from (5.7) and (5.8).

Theorem 2: Assume that $(S^*, R^*) \in H^{s-1}(\Omega) \times H^{s+1}(\Omega)$ $(s \geq 2)$. Then, the following error estimate holds between this solution and the discrete solution (S_K^*, R_K^*).

$$\|S^* - S_K^*\|_{H^{\frac{3}{2}}(\Omega} + \|R^* - R_K^*\|_{H^1(\Omega)} \leq C h^s \left(\|S^*\|_{H^{s-1}(\Omega} + \|R^*\|_{H^{s+1}(\Omega} \right) \quad (5.9)$$

This estimate is optimal and proves the good properties of our discretisation.

Numerical Implementation

In this section, some examples of applications of the proposed model are explored. For that purpose, we consider a bioactive glass scaffold with a certain microstructure immersed in an infinite S medium. Samples I, II and III

are used and different parameters choices are analysed. The process of dissolution and bioactivity is explicitly modelled in the present work. Other authors have provided results by means of the Voxel -FEM methodology, see for example [14]. To control the physical features of this complicated process, here we use a finite volume scheme and the open source FreeFem++ software to solve (5.2) or (5.3). The numerical procedure to solve the proposed model is summarized in the following algorithm:

Algorithm

1. Initialize variables with node values $S^*_{t=0} = 1$, $R^*_{t=0} = 0$ and $B^*_{t=0} = B^*_0$
2. Compute B^* from (4.6) by considering $H[B^*] = 1$
3. Consider $H[B^*] = 1$ and compute s^* and R^* from (5.3) using (4.10)
4. If B^* becomes < 0 for the component i of the vector, then goto 3. with $H[B^*] = 0$

For the degradation we use the indicator defined by

$$Deg(\%) = 100\left(B_0^* - \frac{1}{V_0}\int_{V_0} B(t)dV_0\right), V_0 \text{ is the initil volume.} \tag{5.10}$$

For numerical implementation, we have chosen cases that correspond to the analysis of the most important model parameters for bioactivity and biomaterial degradation for different cases with initial concentrations $S^*_0 = 1$ and $B^*_0 = 1$. To solve the system of equations ((4.6)-(4.7)) together with the initial conditions (4.4) and the boundary conditions (4.8) and(4.10), we consider a finite difference and a finite volume schemes for the time and the space variable discretisations, respectively. It should be pointed out that the disappearance, and new layer formation, due to the dissolution process, can be easily simulated by removing and adding elements, respectively. By applying the above algorithm, we get the numerical results resumed in Figures 2 and 3. Here we consider a particular finite volume scheme, for more details the reader is referred to Nouri section 3 [11].

Results and comments

We consider a bioactive glass scaffold with a certain microstructure immersed in an in finite S medium. Un example of application is a particular type of micro architecture usually found in scaffolds fabricated by means of a porogens (Diego *et al*., 2007, [4]), is represented by the microstructure of 1/8 of a spherical biomaterial (scaffold) containing a hole, as shown in Figure 2. A priori, any bioactive material may be analysed just fitting the model parameters, namely, molar coefficients M_{sd}, M_b, M_{rd}, may be obtained by analysing the chemical reagents involved in the reactions, whereas the diffusion coefficients Ds and Dr can be set according to Fickean experiments for the simulated body fluid and reactant, respectively, within the biomaterial. Obtaining model parameters requires experimental setup for each specific biomaterial. However, these tests are done with respect to well-established standard protocols. As a first simplified approach, we consider $M_{sd} = M_b = M_{rd} = 1$ and assume that $D^*_s = D^*_r = D^*$ by exploring two cases with $D^* = 0.003$ and $D^* = 0.0003$ (i.e.10 times smaller) together with two diffusion rate constants $k_d = 2$ and 4 (i.e.twice larger). Furthermore, we assume the formed HA layer to be impermeable and therefore null diffusion in this part of the domain occurs. First a sensitivity analysis to D^* is performed according to the chosen parameters to simulate dissolution and bioactivity. Secondly, we plot the errors derived from the proposed scheme. Results are presented as follows:

1. In Figure 2, an actual bioglass scaffold microstructure (scaffold with a hole) is numerically reproduced in order to simulate a realistic example of dissolution, and solutions to system (5.2) are shown in Figure 3.
2. The biomaterial is assumed to be immersed in the solution S, boundary (applied on the symmetry planes) together with initial conditions. We consider the following selected cases:

1. case 1: $D^* = 0{:}003$; $k_d = 4$
2. case 2: $D^* = 0{:}003$; $k_d = 2$
3. case 3: $D^* = 0{:}0003$; $k_d = 4$
4. case 4: $D^* = 0{:}0003$; $k_d = 2$

and results are resumed in Figure 4, showing the degradation evolution from equation (5.10).

3- Figure 5 presents the error analysis for the finite volume scheme i.e. error plot from (5.7), (5.8) and (5.9).

The selected cases correspond to the analysis of the most important model parameters for bioactivity and biomaterial degradation. The diffusion parameter D^* references to aqueous species transport within the biomaterial which may be readjusted, to some extent, controlling biomaterial micro porosity and cracks formation during scaffold fabrication.

Conclusion

The bioactivity and dissolution of the bioactive glass (SiO_2-CaO-P_2O_5) has been mathematically and numerically studied. The mathematical model is posed at the continuum level and is rationally based on the most fundamental chemical equations, identifying generic species involved in the phenomenon of bioactivity and glass dissolution. Biomaterial structure evolution, as a result of both dissolution and bioactivity, has been simulated using the finite volume method that provides a robust and efficient technique to simulate structure evolution of complex geometries. This may provide a useful platform as a contribution to test biodegradation and

bioactivity of bioglass-based scaffolds, which are an active and promising area of research of biomaterials for regenerative medicine fields, such as bone tissue engineering and pharmacology to search for prolonged-release drugs. Note that this simplified model is considered by neglecting ionic species, through the stoichiometric coefficients of the variables O_d in equation (3.1). These variables can be added but this will increase the model parameters to be fitted. As an approximate approach, is to fit an average molar content and average kinetic equation.

Acknowledgements: We are grateful to URASM and ENSMM for the help provided to realise our experimental work

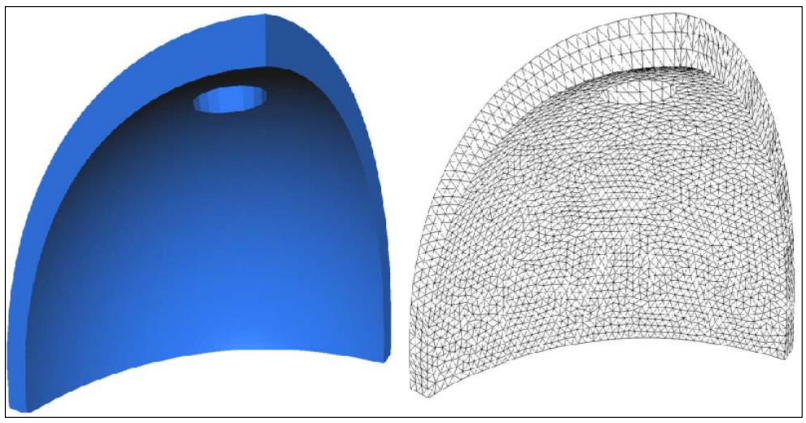

Fig 2: Bioactive glass scaffold and its meshing

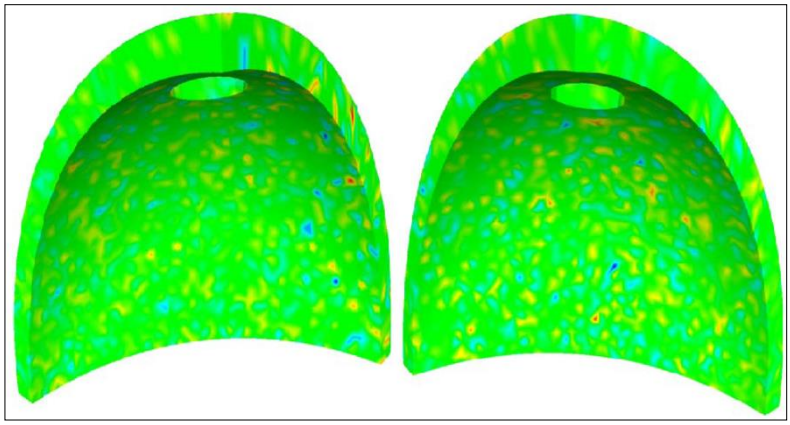

Fig 3: The concentrations S (left) and R (right) solutions of (5.2)

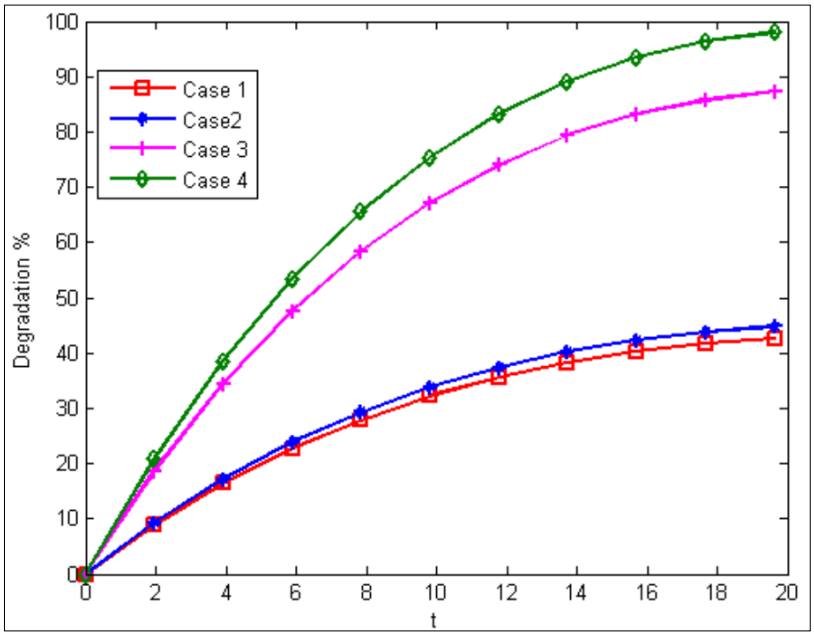

Fig 4: Degradation evolution from equation (5.10) for the four cases

References

1. Assala N Djedaidi, Nouri FZ. Dynamical behaviour of miscible fluids in porous media, International Journal of Dynamical Systems and Differential Equations (IJDSDE),2018:8(3):190-203.
2. Michelina Catauroa, Alessandro Dell' Erab, Stefano Vecchio Cipriotic. Synthesis, structural, spectroscopic and thermoanalytical study of sol{gel derived SiO2{CaO{P2O5 gel and ceramic materials, Thermochimica Acta,2016:625:20-27.
3. Chen QZ, Thouas GA. Fabrication and characterization of sol{gel derived 45S5 Bioglass registered{ceramic scaffolds, Acta Biomaterialia,2011:7(10):3616-3626.
4. Diego RB, Mäs-Estellès J, Sanz JA, Garcia-Aznar JM, Salmerön-Sanchez M. Polymer scaffolds with interconnected spherical pores and controlled architecture for tissue engineering Fabrication, mechanical properties and finite element modeling, J. Biomed. Mater. Res. B,2007:81:448-455.
5. Gupta R, Kumar A. Bioactive materials for biomedical applications using sol{gel technology, Biomed. Mater,2008:3(3):034005.
6. Aymen Hadji, Abdelali Merah, Ouanassa Guellati, Mohamed Guerioune. Synthesis and characterization of the bioactive ternary SiO_2-CaO-P_2O_5 Bioglass, International Journal of Engineering and Applied Sciences, 2018:5(2):23-28. (IJEAS), ISSN: 2394-3661.
7. Hench LL, Splinter RJ, Allen WC, Greenlee TK. Bonding mechanism at inter-face of ceramic prosthetic materials, J. Biomed.Mater. Res,1972:2:117-141.
8. Innocenzi P. Infrared spectroscopy of sol{gel derived silica-based lms: aspectra-microstructure overview, J. Non-Cryst. Solids,2003:316:309-319.
9. Martin RA, Yue S, Hanna JV, Lee PD, Newport RJ, Smith ME *et al*. Characterizing the hierarchical structures of bioactive sol-gel silicate glassand hybrid sca olds for bone regeneration, Philos. Trans. R. Soc. A,2012:370:1422-1443.
10. Nouri FZ. A New Approach for a Multiphase Flow Problem, Int. J. of Mathematics and Computation,2019:30(3):32-42.
11. Nouri FZ. A Review on Multiphase Flows and Applications, Rev. Sci. Technol., Synthèse, Rev. Sci. Technol., Synthse,2021:27(1):1-14.
12. Papadopoulos C, Kantiranis N, Vecchio S, Lalia-Kantouri M. Lanthanidecomplexes of 3-methoxy-salicylaldehyde, J. Therm. Anal. Calorim,2010:99:931-938.
13. Pourhashem S, Afshar A. Double layer bioglass-silica coatings on 316L stainless steel by sol{gel method, Ceram. Int,2014:40(1):993-1000.
14. Sanz-Herrera JA, Boccaccini AR. Modelling bioactivity and degradation of bioactive glass based tissue engineering scaffolds, International Journal of Solids and Structures,2011:48:257-268.
15. Shih CJ, Lu PS, Hsieh CH, Chen WC Chen JC. Effects of bioglass powders with and without mesoporous structures on broblast and osteoblast responses, Appl. Surf. Sci,2014:314:967-972.
16. Van Noorden TL, Pop IS. A Stefan problem modelling crystal dissolution and precipitation, IMA J. Appl. Math,2008:73:393-411.
17. Wang Y, Pan J, Han X, Sinka C, Ding LA. Phenomenological model for the degradation of biodegradable polymers, Biomaterials,2009:29:3393-3401.